EARTH SURFACE PROCESSES AND LANDFORMS
Earth Surf. Process. Landforms **41**, 240–255 (2016)

Published online 12 October 2015 in Wiley Online Library
(wileyonlinelibrary.com) DOI: 10.1002/esp.3842

Metrics for quantifying anthropogenic impacts on geomorphology: road networks

Giulia Sofia,* Francesco Marinello and Paolo Tarolli
Department of Land, Environment, Agriculture and Forestry, University of Padova, Legnaro (PD) Italy

Received 19 December 2014; Revised 8 September 2015; Accepted 8 September 2015

*Correspondence to: Giulia Sofia, Department of Land, Environment, Agriculture and Forestry, University of Padova, Agripolis, viale dell'Università 16, 35020 Legnaro (PD), Italy. E-mail: giulia.sofia@unipd.it

ESPL
Earth Surface Processes and Landforms

ABSTRACT: This work tests the capability of a recently published topographic index, the Slope Local Length of Auto-correlation (SLLAC), to portrait and delineate anthropogenic geomorphologies. The patterns of the anthropogenic pressure are defined considering the road network density and the Urban Complexity Index (UCI). First, the research investigates the changes in the SLLAC in two derived parameters (average SLLAC and the SLLAC surface peak curvature – Spc – per km^2) connected to the increasing of the anthropogenic structures. Next, natural and anthropogenic landscapes are clustered and classified. The results show that there is a direct correlation between the road network density and the UCI, and the mean SLLAC per km^2. However, the Spc is inversely correlated with the anthropogenic pressure (network density and urban complexity). This shows that the surface morphology (slope) of regions presenting anthropogenic structures tends to be well organized (low Spc) and, in general, self-similar at a long distance (higher average SLLAC). The results of the clustering approach show that the procedure can correctly depict anthropogenic landscapes having a road network density greater than about 3 km/km^2, also in areas covered by vegetation. This latter result is promising for the use of such a procedure in regions that cannot be seen directly from orthophotos or satellite images. The proposed method can actively capture the alteration produced by road networks on surface morphology identifying different signatures of urban development: exploration and densification networks that are responsible for increasing the local density of the network and expanding the network into new areas, respectively. The effects of this alteration on surface processes could be significant for future research, creating new questions about differences due to human or landscape forcing on Earth surface processes. Copyright © 2015 John Wiley & Sons, Ltd.

KEYWORDS: landscape; LiDAR; SLLAC; anthropogenic signatures; road networks; geomorphology

Introduction

Environmental planning and management at the landscape level have become the main focus of many studies (Sheppard, 2000), and numerous researchers underlined how landscapes spanning over tens or hundreds of square kilometres are relevant geographic domains for dealing with ecological, environmental and geomorphological topics (Wu and Qi, 2000; Ellis *et al.*, 2013). The Anthropocene for geomorphologists has been widely discussed (i.e. Lewin and Macklin, 2014), and there is enough geomorphological evidence to support the idea that human activities have become the dominant drivers in many Earth surface fluxes at different scales (Steffen *et al.*, 2007; Wohl, 2013). Furthermore, the impacts of these forcing activities are likely to continue into the future and be preserved in long-term geological records, at least in some environments (Zalasiewicz *et al.*, 2011; Brown *et al.*, 2013; Jefferson *et al.*, 2013). Today, humans are among the most prominent geomorphic agents (Hooke, 2000; Cots-Folch *et al.*, 2006), redistributing the Earth surface for urbanization through filling, grading, mining, and terracing, causing drastic changes to the geomorphic organization of the landscape (Jones *et al.*, 2014). The consequences of such, among others, are land degradation (Tarolli, 2014; Tarolli *et al.*, 2015) and changes in the hydrologic response (Brath *et al.*, 2006). The geomorphic impact of human activities is so prominent that researchers defined specific disciplines, such as the 'urban geomorphology' (Coates, 1984), 'anthropogeomorphology' (Cuff, 2008) or 'anthropogenic geomorphology' (Szabo, 2010), where humans are studied as an agent of change with mutual feedback mechanisms in the land–water ecosystem. The surface of the Earth is being transformed by technological systems and processes that move significant quantities of soil (Haff, 2010), and the relief is modified to the needs of urban development or for agricultural purposes (Ahnert, 1988). In addition, road networks strongly shape the pattern of territories (Borruso, 2003). A series of ecological impacts of roads involving, for example, influences on species, soil development and the water cycle, has been identified. These impacts vary in distance outward from metres to kilometres, to the point that some researchers define a 'road-effect zone' (Forman, 2000; Forman *et al.*, 2003), where near natural ecosystems are close enough to face the earlier-mentioned road effects. Further, roads create problems associated with erosion and sediment production (Reid *et al.*, 1981; Luce and Cundy, 1994; Montgomery, 1994; Tarolli *et al.*, 2013), and landslide hazards

(Gucinski *et al.*, 2001; Sidle and Ziegler, 2012; Penna *et al.*, 2014). Gully erosion on the hillslopes can be significantly influenced by the building of the road itself (Nyssen *et al.*, 2002), or by the concentration of surface runoff and the rearrangement of drainage pathways along the road's surface (Katz *et al.*, 2014).

The reconstruction or identification of anthropogenic topographies provides a mechanism for quantifying anthropogenic changes to the landscape systems in the context of the Anthropocene epoch (Jordan *et al.*, 2014). Land managers [to follow for example the European Commission's regulations (2000, 2012)] and researchers have indeed called for the development of cost-effective and flexible methods for the identification and monitoring of anthropogenic features starting from data from different sources, focusing on elements such as terraces, roads, open-pit mines, river banks or artificial drainage networks (Carluer and Marsily, 2004; Krause *et al.*, 2007; Collins *et al.*, 2010; Passalacqua *et al.*, 2012; Cazorzi *et al.*, 2013; Tarolli *et al.*, 2013; Hailemariam *et al.*, 2014; Sofia *et al.*, 2014a; Prosdocimi *et al.* 2015; Chen *et al.* 2015).

The current ability to track, quantify and predict human-induced geomorphic changes is hindered by insufficient data and reliance on methodologies developed for traditional geomorphic studies in natural settings (Djokic and Maidment, 1991; Gironás *et al.*, 2009; Haff, 2010; Rózsa, 2010; Szabo, 2010). High-resolution topographic data, such as light detection and ranging (LiDAR) among others, offer new opportunities to better understand geomorphic processes, especially in engineered landscapes where the direct anthropic alteration of processes is significant (Tarolli, 2014). Recently, literature underlined the effectiveness of high-resolution topography in identifying anthropogenic features (i.e. Passalacqua *et al.*, 2012; Sofia *et al.*, 2014a; Chen *et al.* 2015), and analysed their effects on earth surface processes in numerous environmental contexts (Jones *et al.*, 2014; Tarolli *et al.*, 2013; Tarolli *et al.*, 2015).

This work will describe a method for identifying human-modified geomorphic landscapes using LiDAR digital terrain models (DTMs). The procedure is based on a recently published topographic metric, the Slope Local Length of Auto-correlation (SLLAC) (Sofia *et al.*, 2014b), to highlight characteristic geomorphic signatures of the urbanization process left by the construction of road networks and urban areas. The present research can be divided into three parts. First, the SLLAC and some derived parameters will be analysed in relation to anthropogenic elements such as road network density and urban area complexity (number of buildings and road junctions). Next, the indices will be used to detect automatically anthropogenic landscapes. Finally, the future challenges, current capabilities and possible utilizations will be highlighted.

Methodology

Slope local length of auto-correlation (SLLAC) computation

Landscapes result from numerous processes that interact spatially and temporally. It is well known that urbanization modifies the traditional landscape, creating complex and diverse landscapes consisting of a highly fragmented mosaic of different forms of land cover and a dense transport infrastructure. Natural landscapes have varying behaviours at different scales, and, at the same time, morphology has varying statistical behaviours from place to place. Drăguţ *et al.* (2011) underlined how homogeneous areas that convincingly associate into patterns of land-surface parameters are well differentiated across scales. Sofia *et al.* (2013) showed that the change in statistics at the changes in computational scale can be read as a signature of channelized morphologies. This was also confirmed by Sofia *et al.* (2015) using field surveyed data.

At the landscape scale, natural elements, such as coastlines and river networks, present a self-similarity that is typically fractal-like (Tarboton *et al.*, 1988; Rodriguez-Iturbe and Rinaldo, 1997). However, at a smaller scale, landforms could be differently influenced by landscape forcings (e.g. biota, Dietrich and Perron, 2006), and they could result in characteristic forms that break the typical self-similar scaling of (un-vegetated) morphologies (Baas and Nield, 2007). Consequently, the landscape typically exhibits complex, apparently random behaviours and patterns in the spatial (and temporal) domain (Phillips, 1992). Therefore, at a local scale, natural morphologies (thus, slopes) are expected to change rapidly: natural areas are inherently irregular, and neighbouring areas can exhibit low correlations. However, artificial surfaces typically show a reduced variability to fulfil human needs for mobility and machine access (Sofia *et al.*, 2014b). Some authors also pointed out how the morphology of the built-up (anthropogenic) environment is quite constant and – on average – quite independent of its shape (Thomas *et al.*, 2008). At the local scale, anthropogenic slopes and surface morphology are expected to demonstrate high levels of self-similarity with neighbouring areas. Sofia *et al.* (2014b) proposed to characterize surface morphologies by focusing on local slope similarities and to quantify these similarities in terms of length of correlation. In this work, we decided to enlarge this view to other anthropogenic elements such as roads and urban footprints. The change in slope between a road surface, berm or shoulder and the surrounding landscape is, in fact, quite typical, independent of the size of the road: the same could be said about urban footprints.

The SLLAC calculation begins with the evaluation of the magnitude of the slope determined locally, starting from the DTM, as

$$\text{Slope} = \sqrt{f'^2_x + f'^2_y} \tag{1}$$

where f'_x and f'_y are partial derivatives of a bivariate function $Z = f(x,y)$ representing the elevation of the bare ground (in this case). There are multiple algorithms for the definition of Z; however, quadratic-based polynomial models, such as the Evans (1972, 1979) approach, give more stable results in geomorphological applications (Schmidt *et al.*, 2003).

The SLLAC is obtained using a moving window (kernel) approach with two steps for each kernel (Figure 1): (i) calculating the correlation (Equation 2) (Figure 1b) between a squared slope patch (also referred as template) (T in Figure 1a) and the window (kernel) containing the patch (W in Figure 1a); (ii) identifying the characteristic length of correlation (Figure 1c).

The correlation (Figure 1b) $\text{Corr}_{(i,j)}$ is computed according to the procedure proposed by Haralick and Shapiro (1992) and Lewis (1995) as:

$$Corr_{(i,j)} = \frac{\sum_{u,v}\left(W_{(i+u,j+v)} - \overline{W}_{i,j}\right)\left(T_{u,v} - \overline{T}\right)}{\left(\sum_{u,v}\left(W_{(i+u,j+v)} - \overline{W}_{i,j}\right)^2 \sum_{u,v}\left(T_{u,v} - \overline{T}\right)^2\right)^{0.5}} \tag{2}$$

Assuming a kernel W having a size $M \times M$, and a slope template T of size $N \times N$ (Figure 1), indices (i,j) are the row and column position of each pixel within the kernel and they are valid in $1 \le i \le (M-N)$ and $1 \le j \le (M-N)$, while indices (u,v) run across $1 \le u \le N$ and $1 \le v \le N$. Thus $\overline{W}$ is the local mean slope of the kernel W underneath the slope patch T whose top left corner lies on pixel (i,j), and $\overline{T}$ is the mean value of the slope patch.

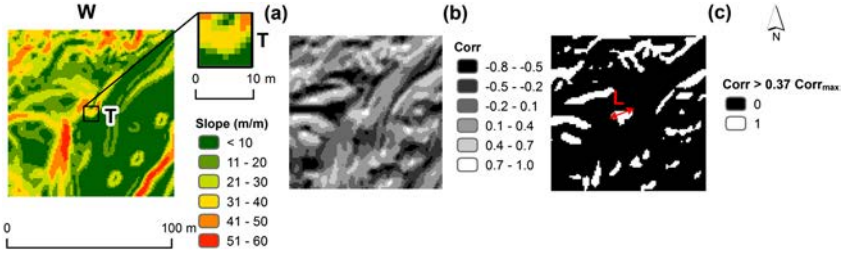

Figure 1. Example of the calculation of SLLAC for a single moving window (W). (a) For each moving window (W), a slope template (T) is identified, having the centre at the centre of W. The cross-correlation between T and W is computed (b), and the resulting map is thresholded at 37% of its maximum value (c). The length of correlation is then the length of the longest line passing through the central pixel and connecting two boundary pixels on the extracted area connected to the central pixel. This figure is available in colour online at wileyonlinelibrary.com/journal/espl

The correlation length is defined as the horizontal distance of the correlation function (CF), which has the fastest decay to a specified value s, with $0 \leq s < 1$ (ISO, 2013a, 2013b). In a one-dimensional (1D) correlation, the choice of s is generally set between 10% and 50% of the correlation original value, but this is rather arbitrary (Whitehouse, 2011). In general, to be independent from the complexity of the CF, the length should be defined where the envelope of the function falls to a lower level than 1/e (~0.37) (Whitehouse, 2011). Equation 2 defines a two-dimensional (2D) correlation that varies between −1 and 1; for this function, the correlation length is defined using a threshold on the cross-correlation map (Figure 1b) corresponding to 37% of its maximum value (Sofia *et al.*, 2014b) (Figure 1c), and focusing only on the extracted area connected to the central pixel. The correlation length is the length of the longest line passing through the central pixel of the kernel W, and connecting two boundary pixels on the extracted area (Figure 1c) (Sofia *et al.*, 2014b).

The SLLAC map can be further analysed using the Spc (surface peak curvature) parameter that is based on a second derivative calculation: it provides an indication of the tri-dimensional variability of a dataset (Stout *et al.*, 1994). Sofia *et al.* (2014b) and Chen *et al.* (2015) showed that the higher the Spc, the lower the coverage of anthropogenic features in the area.

The Spc is defined as:

$$Spc = -\frac{1}{2n}\sum_{i=1}^{n}\left[\left(\frac{\partial^2 F_{(c,r)}}{\partial^2 c}\right) + \left(\frac{\partial^2 F_{(c,r)}}{\partial^2 r}\right)\right]_i \qquad (3)$$

where n is the number of considered peaks, i indicates that the quantity between brackets is computed for each peak, F corresponds to the analysed map value (in this case, the SLLAC map), and c and r represent cell spacing in every direction. A peak is defined as a pixel where all eight neighbouring pixels are lower in value (Stout *et al.*, 1994).

In addition to the Spc, we also analysed the mean SLLAC value ($\overline{\text{SLLAC}}$) to test if this statistic can also differentiate natural landscapes from artificial ones.

In general, the correlation value (Equation 2) always varies between −1 and 1, depending on the similarity between the slope patch and the analysed neighbourhood, and it does not depend on the size of the patch T or of the kernel W, and it. The highest correlation value (Corr = 1) will be found at the centre of W, where the slope patch is located, but areas having a slope conformation similar to the template will display high correlation values as well. What depends on the size of the cross-correlation matrix is the maximum measurable correlation length. Given the circular constraint of the method (Sofia *et al.*, 2014b), the maximum length that can be found is equal, at most, to $M + N - 1$. In general, the size of the template T should be wide enough to capture at least the change of slope between the road berm/road shoulder and the surrounding landscape or the changes between the border of the footprint of a building and the area around it. However, because the procedure applied uses a moving window, the template does not need to capture the whole width of the road/building; by moving the window, we can detect any element, as long as it is present on the DTM.

Figure 2 shows values of the Spc (Equation 3) (Figures 2a and 2c) and average SLLAC (Figures 2b and 2d) computed for two areas (one natural and one anthropogenic) considering a square slope template (T) having widths of 10 to 30 m and a fixed window of 100 m (Figures 2a and 2b), and a fixed template of 10 m and different windows (W) having sizes of 100 to 300 m (Figures 2c and 2d).

When changing the sizes of the slope patch and the slope template, the magnitude of the Spc is what changes, but the differences in the SLLAC parameters tend to remain constant (higher Spc for natural surfaces, lower Spc for anthropogenic ones). However, when changing the size of the template T (Figures 2a and 2b), the difference in the average SLLAC remains until the template size is smaller than W/4 (in the figure, until T is smaller than 25 m). This issue is related to the Lewis (1995) approach. This method assumes that the template is small compared to the image, and proceeds to calculate the normalization across the entire template. This leads to correct computations wherever the template is wholly overlapping the kernel, but the computation is incorrect in the borders of the output (the border size is proportional to the template size). Therefore, this problem is worse for larger templates because, when the template is the same size as the kernel W, the only correct value is at the central pixel (where the kernel and the template fully overlap). Clearly, at the increasing of the size of T, the border effect is larger and it masks the morphology effect. From this short example, it appears that (a) changes in W have generally no influence on the differences between anthropogenic and natural morphologies; (b) changes in T have more of an impact. However, as long as the size of T < W/4, the difference between anthropogenic and natural morphologies remains. Further, Sofia *et al.* (2014b) showed that increasing the size of the windows results in an increase in the computational time. We suggest to consider the SLLAC derived parameters as a relative measure. We also suggest not to use the magnitude of the Spc or the SLLAC as absolute values, but rather to compare differences within the same study site (see later). Considering these reasons, the measures of the patch and the kernel in this study case are set as those in Sofia *et al.* (2014b): 100 m × 100 m for the kernel W, and 10 m × 10 m for the template T.

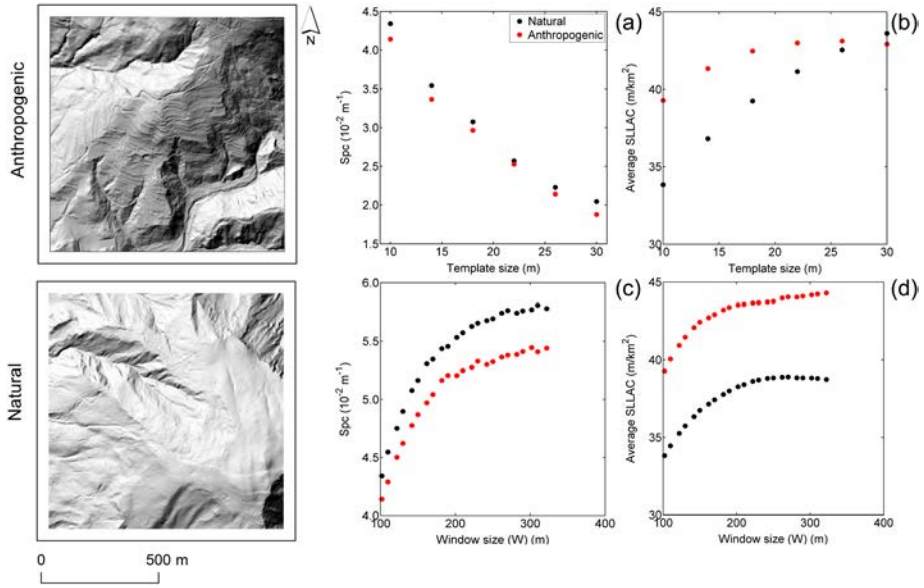

Figure 2. Values of Spc (Equation 3) (a and c) and average SLLAC (b and d) computed for two areas (one natural and one anthropogenic) considering a square slope template (T) having widths of 10 to 30 m and a fixed window of 100 m (a and b), and a fixed template of 10 m and different windows (W) having sizes of 100 to 300 m (c and d). This figure is available in colour online at wileyonlinelibrary.com/journal/espl

In this study, the SLLAC is computed over wide areas (in the orders of tens of square kilometres), and, in a second step, the Spc and the SLLAC are computed using a square moving window of 1 km^2, therefore providing an analysis of the two parameters in m/km^2 and m^{-1}/km^2. Ellis and Ramankutty (2007) and Ellis *et al.* (2010) categorized human/ecosystem interactions into classes based on population density per km^2. In addition, as a general rule of thumb in surface metrology (Khonsari and Booser, 2008), the analysed area, in order to be significant, should be at least 5–10 times the size of the considered filters. If we can generalize such a concept, and we consider the size of W as the size of the considered filter, we recommend using a moving window about 10 times the size of W.

Anthropogenic landscape characterization

In this work, any location on a map that presents anthropogenic structures (buildings) or a road network is considered anthropogenic. Transport networks, in fact, show the patterns of anthropic activities at regional and local levels; the proportion of space occupied by roads increases as centres of activity are approached, and the proportion of space occupied by roads decreases with increasing distance from the main urban areas (Haggett and Chorley, 1996). At the same time, the growth of urban areas and road networks is generally governed by two elementary spatial processes, densification and exploration, which are responsible for increasing the local density of the network and expanding the network into new areas, respectively (Forman *et al.*, 2003; Strano *et al.*, 2012; Corcoran *et al.*, 2013). The exploration is characterized by sparse buildings and long roads connecting separated areas, while the densification is characterized by dense networks made of short branches with sharp angles. A first analysis, therefore, considers the Spc and the $\overline{\text{SLLAC}}$ in relation to the road network density (in km/km^2). For this purpose, the network density is calculated as total length per unit area from road features, available online from OpenStreetMap (OpenStreetMap, 2014). A further investigation includes an analysis of an Urban Complexity Index (UCI) (in pts/km^2), computed with point data for the junctions of the road network and the number of buildings. The UCI was inspired by Borruso (2003), where the street number density provided a physical index of the urban built environment. For our analysis, we argue that the number of road junctions and buildings can be a good index of the complexity of the urban system/road network; therefore, we deemed it interesting to analyse this parameter in relation to the SLLAC. Both indices are based on the quadratic Kernel Density Estimation (KDE) to obtain smooth continuous surfaces from the sets of points or linear features (Gatrell, 1994). In this case, the KDE is based on the kernel function described by Silverman (1988). The only arbitrary variable in the KDE is represented by the bandwidth (Gatrell, 1994), but Borruso (2003) showed that a bandwidth of 500 m provides optimal results for the identification of urban areas. In this case study, we checked and confirmed that the use of this bandwidth provided measures of the parameters that, on average, were closely related (with differences $< 0.01\%$) to the actual total network density (computed as the ratio between the road network length and the area of the study site) and the total point density (ratio between the number of points – buildings and junctions – and the area of the study site). To identify characteristic relationships between the SLLAC derived parameters (Spc and SLLAC), the road network density and the UCI, we simply tested their dependency in terms of the Pearson's correlation coefficient (Pearson, 2006), which is widely used in science as a measure of the degree of linear dependence between two variables.

As a further step, the overall shape of the network was defined by the ratio between the road network density and the UCI (Network Simplicity – NS). The NS can potentially range from zero for areas having no network (only isolated buildings), up to infinity where there are long roads with no junctions or buildings. Densification networks are expected to have a lower NS value, being characterized by a high network density and, at the same time, a very high number of junctions and buildings. Exploration networks are characterized by a higher NS value (network density might be comparable to that of the densification networks, but the network is composed of longer roads with a lower number of junctions, and urban areas present fewer buildings).

Automatic detection of anthropogenic morphologies

When considering the correlation length value (thus, the $\overline{\text{SLLAC}}$) at a local scale, anthropogenic morphologies are expected to be self-similar at a longer distance (high $\overline{\text{SLLAC}}$) than that of a natural morphology (Sofia *et al.*, 2014b). However, the creation of anthropogenic morphologies also implies a different organization of the landscape; the Spc defines if the fibres of the SLLAC maps are wide, organized and aligned creating plateaus (low values of the Spc), or if they are randomly placed on a noisy background (high value of the Spc) (Sofia *et al.*, 2014b). An area that has a well-organized morphology will likely have a low Spc. Morphologies that are self-similar at long distances are likely to have a high $\overline{\text{SLLAC}}$. More complex anthropogenic areas, with networks having short roads and many junctions, and urban areas with many buildings (Figures 3b and 3e), are likely to be self-similar at a distance shorter than that of a terrace or a long isolated road (Figures 3a and 3d); however, they would display a higher organization in the landscape with respect to a natural landscape (Figures 3c and 3f).

Therefore, surfaces that simultaneously minimize the Spc and maximize the $\overline{\text{SLLAC}}$ are self-similar at long distances, but, at the same time, present a clear organization of the fibres (for example, the ones displayed in Figures 3a and 3d). Areas that minimize the Spc in alternation to maximizing the $\overline{\text{SLLAC}}$ are either well organized (Figures 3a and 3b) or less organized, but self-similar at a longer distance (Figure 3a), or both.

Given these premises, to label the anthropogenic areas once the maps of $\overline{\text{SLLAC}}$ and Spc are computed, we applied a *k*-means clustering algorithm to partition each dataset into two main categories (natural versus anthropogenic) (Figure 4).

The *k*-means clustering, for its simplicity and speed, is a widely used iterative, data-partitioning algorithm that assigns *m* observations to exactly one of the *k* clusters defined by centroids, where *k* is chosen before the algorithm starts. The algorithm seeks to minimize the average squared distance between points in the same cluster (David and Vassilvitski, 2007). The algorithm proceeds as follows: (1) choose *k* initial cluster centres (centroid) (in this case, two centroids) according to the method used by David and Vassilvitski (2007); (2) compute point-to-cluster-centroid distances of all observations to each centroid; (3) individually assign observations to a different centroid if the reassignment decreases the sum of the within-cluster, sum-of-squares point-to-cluster-centroid distances; (4) compute the average of the observations in each cluster to obtain *k* new centroid locations; (5) repeat steps 2 through 4 until cluster assignments do not change. For further details, see David and Vassilvitski (2007) and Lloyd (2006).

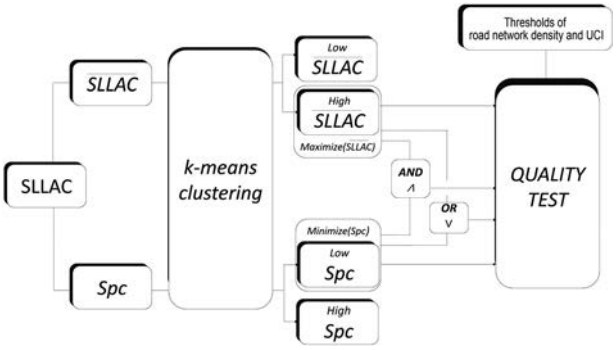

Figure 4. Schematization of the procedure for the delineation of anthropogenic areas.

After the clustering, four hypotheses were tested (Figure 4):

a. maximize ($\overline{\text{SLLAC}}$): anthropogenic landscapes are the cluster having the highest $\overline{\text{SLLAC}}$ implying that anthropic modification of surface morphologies creates areas that are more similar to the others (longer correlation length).
b. minimize (Spc): anthropogenic landscapes are the cluster with the lowest Spc [following Sofia *et al.* (2014b)];
c. maximize ($\overline{\text{SLLAC}}$)$\wedge$ minimize (Spc) where $\wedge$ is the Boolean operator 'AND': anthropogenic landscapes are characterized by a high self-similarity and a high degree of order; hence, they are the cluster that verifies both (a) and (b) in a logical conjunction that results in true if (a) and (b) are simultaneously true;
d. maximize ($\overline{\text{SLLAC}}$) $\vee$ minimize (Spc) where $\vee$ is the Boolean operator 'OR': anthropogenic landscapes are characterized by a high self-similarity, a high degree of order or both; hence, they are the cluster that verifies either (a) or (b) in a logical disjunction that results in true whenever we have a high mean SLLAC, a low Spc or both.

The anthropogenic areas detected according to the points (a) to (d) have been tested against different thresholds of the road network density and of the UCI, considering an overall quality (Heipke *et al.*, 1997).

$$\text{Quality} = \frac{\text{TP}}{\text{TP} + \text{FP} + \text{FN}} \tag{4}$$

where the matching extracted areas are defined as true positives (TPs), while the un-matching extractions are considered false positives (FPs). The anthropogenic areas that are not extracted by the method are classified as false negatives (FNs). Quality varies between zero for extraction with no overlap between extracted and observed features and the optimum value of one for extraction where these coincide perfectly (Heipke *et al.*, 1997).

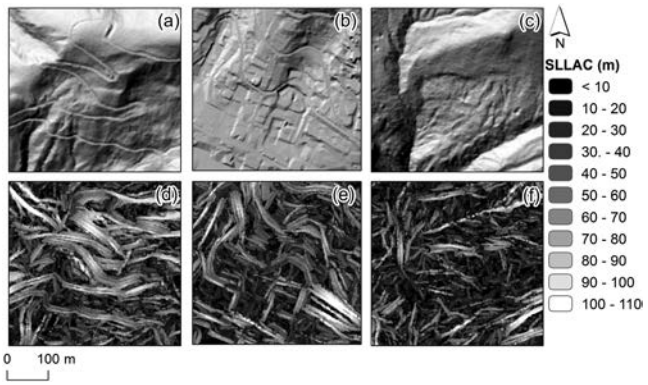

Figure 3. An anthropogenic surface with only one long isolated road (a), and a more complex urban area (b), as compared to a natural area (c). (d)–(f) display the derived SLLAC for each area. Average SLLAC values for the maps on the bottom row are 42.2 m, 41.5 m and 36.8 m, while Spc values are 4.0×10^{-2} m^{-1}, 3.8×10^{-2} m^{-1} and 4.1×10^{-2} m^{-1}, respectively.

Study Areas

We tested the procedure considering LiDAR DTMs coming from different sources and different areas of Europe: three are located in Italy and one is located in Spain (Figure 5). The study areas are referred to as the Trento area (Figure 5a), the Salerno

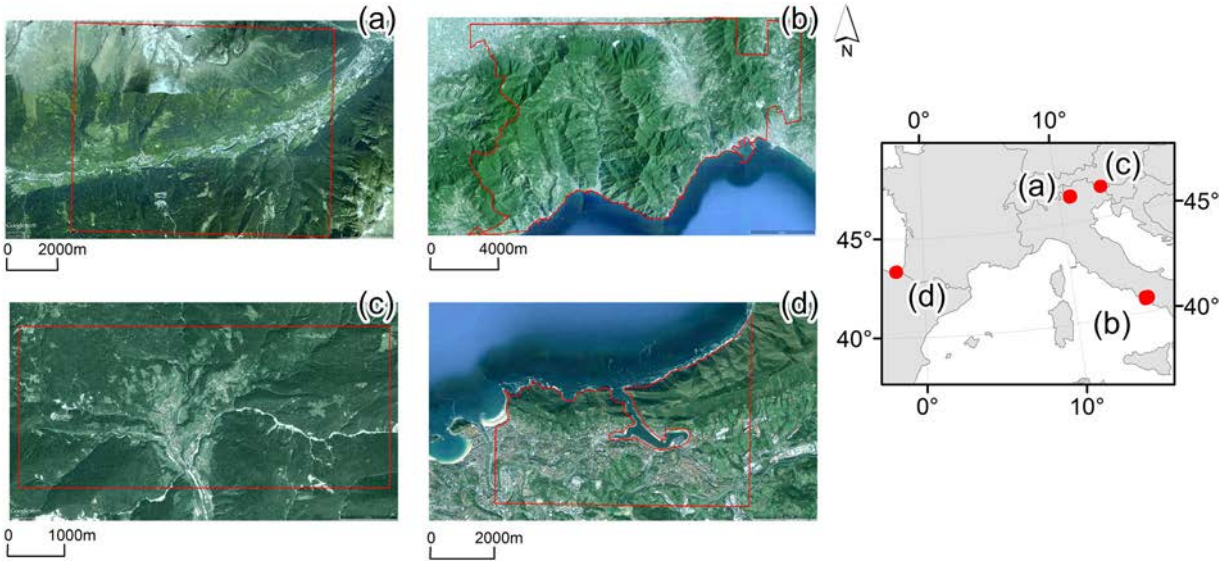

Figure 5. Trento (a), Salerno (b), Paularo (c) and Gipuzkoa (d) study sites. This figure is available in colour online at wileyonlinelibrary.com/journal/espl

area (Figure 5b), the Paularo area (Figure 5c) and the Gipuzkoa area (Figure 5d) after the names of the closest major cities.

The study sites were chosen for different reasons. Sofia *et al.* (2014b) tested the SLLAC procedure in the Alps and in a Mediterranean context. Thus, in the present work, the procedure was tested by generalizing the SLLAC concept to anthropogenic morphologies (road networks and their structure) without introducing an additional variability connected to a change in the overall natural morphology; hence, the choice of the Trento area (Alpine) and the Salerno area (Mediterranean). The other two study sites were chosen for different reasons. The Paularo study site was mainly selected because the effects of roads and trail paths on surface processes were shown by Tarolli *et al.* (2013). The Gipuzkoa area was chosen because the DTMs were freely available for download (Diputacion Foral de Gipuzkoa, 2005): the DTM was randomly selected and downloaded.

The Trento area (Figure 5a) is located in the Italian Alps, more precisely in the Trentino Alto Adige Region. The area is about 80 km^2 wide and presents slopes ranging from 0° to 86° (average 27°) and elevation values ranging from 720 m above sea level (a.s.l.) to 2870 m a.s.l. (average 1498 m a.s.l.). The anthropogenic area is mainly related to the development of small towns (about 1000 inhabitants each) and their road network (about 277 km of roads with an average density of ~3 km/km^2). The study site has an average UCI of ~38 pts/km^2, mostly indicating the presence of a few buildings and long roads: a conformation typical of 'exploration' networks. Other anthropogenic morphologies derive from the terracing system designed for grape cultivation.

The LiDAR dataset for this area is a free download from the Autonomous Province of Trento, and datasets from the same source have already been applied successfully in scientific research (i.e. Cavalli *et al.*, 2013; Sofia *et al.*, 2014b). The considered DTM has a resolution of 2 m per pixel, and presents a vertical accuracy of ±0.15 m for major valleys and urbanized areas, and a vertical accuracy of ±0.3 m for all remaining areas (Cavalli *et al.*, 2013).

The Salerno study area (Figure 5b) is located in southern Italy in the Campania Region, between the municipality of Amalfi on the west side and Salerno on the east side, and is about 177 km^2 wide. Its elevation ranges from 0 to 1300 m a.s.l. (average 400 m a.s.l.), and the slope varies between 0° and 88° (average 27°). Here, the character of urban development is a form of hyper-urbanization, with the proliferation of peripheral housing and the decentralization of the population from the inner city (Pacione, 1987). The anthropogenic surface is mainly connected to the development of the cities of Salerno (the second largest city in the region) and Amalfi. The road network covers about 890 km and has an average density of ~4 km/km^2. The site shows an average UCI of about ~90 pts/km^2, due to the high number of buildings and a more complex road network system within the cities, with numerous short intersecting roads. The conformation of the network in this area is mostly typical of the densification process. However, presenting a large natural area (about 45% of the site), the average UCI and the road network density remain low. The coastal part of the study site shows other anthropogenic morphologies related to terraces for citrus production. The DTM for this area (provided upon request by the Italian Ministry of Environment) exhibits a vertical accuracy of ±0.15 m, and has already been applied successfully in scientific research (i.e. Cazorzi *et al.*, 2013; Sofia *et al.*, 2014a, 2014b, 2014c).

The Paularo study site (18 km^2) is located in northern Italy, in the Friuli Venezia Giulia Region (Figure 5c). The elevation ranges from 600 to 1500 m a.s.l. (average 1000 m a.s.l.), while slope ranges from 0° to 89° (average 29°). The area is characterized by the presence of several villages, roads (57 km with an average density of 3 km/km^2) and activities such as forestry, pasturing and high-altitude farms. The UCI has an average value close to 108 pts/km^2; this high number is mostly due to the number of buildings in the valley bottom. The original LiDAR point cloud had a point density of 2 pts/m^2, and the absolute vertical accuracy of the DTM was estimated to be about 0.3 m (Tarolli *et al.*, 2013). For homogeneity with the other study sites, we generated a reduced-resolution (2 m × 2 m per pixel) version of the Tarolli *et al.* (2013) DTM, where each output cell contained the mean of the input cells that were encompassed by the extent of that cell.

The Gipuzkoa study site (Figure 5d), about 31.5 km^2 wide, is located in Spain, in the Gipuzkoa province, and it is a surrounding area of the capital San Sebastian. The height ranges from 0 to 370 m a.s.l. (average 78 m a.s.l.), while slope ranges between 0° and 85° (average 24°). The anthropogenic surface within the area is mainly due to the development of the city of San Sebastian in the hinterland, as opposed to the wilderness of the coastal area. The road network in this area covers about 517 km and has an average density of

~10 km/km^2. The urban system and the road network are more complex than those of the previous study sites, and the area is characterized by short roads and a very high number of buildings (densification process), determining an average UCI of ~220 pts/km^2. The considered LiDAR data are freely downloadable in tiles of 1 km^2 from the Gipuzkoa web map viewer (Diputacion Foral de Gipuzkoa, 2005). The original LiDAR point cloud had a point density of 2 pts/m^2, with a vertical accuracy of 0.1 m on flat horizontal terrain and a horizontal accuracy of 0.7 m [Institut Cartografic de Catalunya (ICC), 2005, 2008]. The DTMs available for download have a resolution of 1 m per pixel; however, for this work, for homogeneity with the other study sites, we aggregated it to a resolution of 2 m per pixel, using the same approach mentioned for the Paularo DTM.

Results and Discussion

Anthropogenic landscape characterization

Figure 6 shows the SLLAC maps obtained for the four study sites.

Aside from the Gipuzkoa study site (Figure 6d), where two-thirds of the area can be considered anthropogenic, when observing the SLLAC maps of Trento (Figure 6a), Salerno (Figure 6b) and Paularo (Figure 6c), it appears that anthropogenic structures, such as roads, create elongated fibres, similar to the ones showed in Sofia *et al.* (2014b) for terraces. In addition, the presence of urban areas and the footprint of buildings left on the DTMs after the filtering of the point clouds determine higher SLLAC values (i.e. Figure 6c). Figures 7 and 8 show the $\overline{\text{SLLAC}}$ and the Spc values, respectively, which were computed using a 1 km^2 moving window.

After a first visual assessment, it appeared that mountainous natural landscapes had lower values of $\overline{\text{SLLAC}}$ (Figure 7), and higher values of Spc (Figure 8), while anthropogenic areas had higher values of $\overline{\text{SLLAC}}$ and lower values of Spc.

Figure 9 shows scatterplots of the Spc (Figures 9a–9d) and the $\overline{\text{SLLAC}}$ (Figures 9e–9h) related to the road network density for each study site. Figure 10 shows the same comparisons considering the UCI related to the Spc (Figure 10a–10d) and to the $\overline{\text{SLLAC}}$ (Figure 10e–10h). A least-squares line is also shown for each plot.

For both the Alpine study cases (Trento and Paularo), there is a strong direct correlation between the $\overline{\text{SLLAC}}$ and the road network density (Pearson's coefficient was positive and greater than 0.6): the higher the network density, the higher the mean correlation length per km^2 (Figures 9e and 9f). The same (but weaker) correlation can be seen with the UCI (Figures 10e and 10f). The Salerno study site shows the same behaviour; however, the Pearson's coefficient displays a lower value in the case of $\overline{\text{SLLAC}}$ as compared to the road network density, indicating a slightly weaker direct correlation. The Gipuzkoa study site shows almost no correlation between the $\overline{\text{SLLAC}}$, the road network density and the urban complexity (Pearson's coefficient was close to zero and statistically insignificant). This is mainly because some of the areas with low road density and UCI showed peculiar morphological structures that were clearly visible on the DTM, which created elongated fibres on the SLLAC map, resulting in high values of $\overline{\text{SLLAC}}$ (Figure 11).

When analysing the Spc, all study sites showed a strong inverse correlation with road density and UCI (Pearson's coefficient was always smaller than −0.4). The overall inverse correlation between the anthropogenic pressure (road network and urban complexity) and the Spc parameter was in line with Sofia *et al.* (2014b), where the increasing of terraced areas within the study sites resulted in a decrease of the Spc value that was independent of the morphological context of the area. Similar conclusions can be drawn for the $\overline{\text{SLLAC}}$ and the Spc compared to the urban complexity.

Automatic detection of anthropogenic morphologies

Tables I–III show the maximum quality for the extraction hypothesis described earlier, compared to different thresholds of road network density, UCI, and NS, respectively.

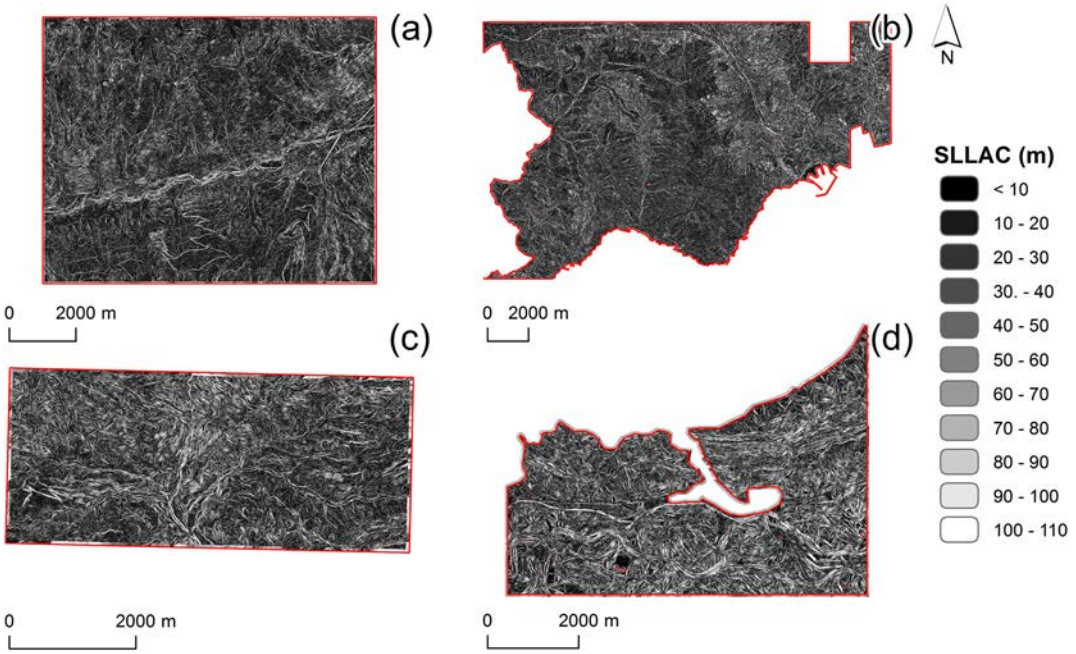

Figure 6. SLLAC map for the Trento (a), Salerno (b), Paularo (c) and Gipuzkoa (d) study sites. This figure is available in colour online at wileyonlinelibrary.com/journal/espl

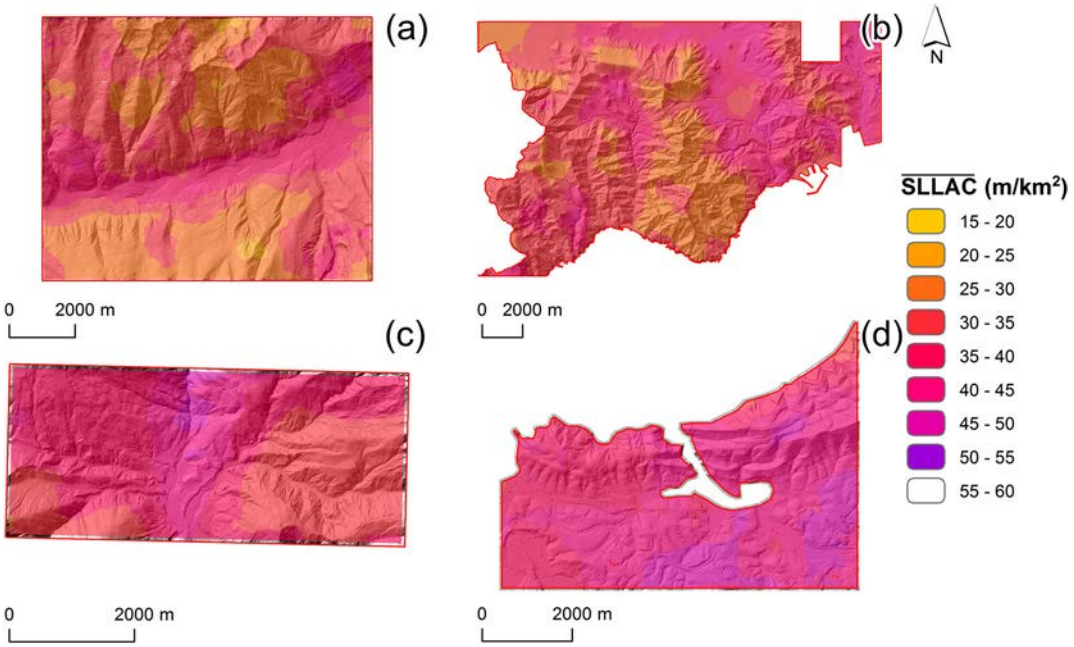

Figure 7. $\overline{SLLAC}$ map for the Trento (a), Salerno (b), Paularo (c) and Gipuzkoa (d) study sites. This figure is available in colour online at wileyonlinelibrary.com/journal/espl

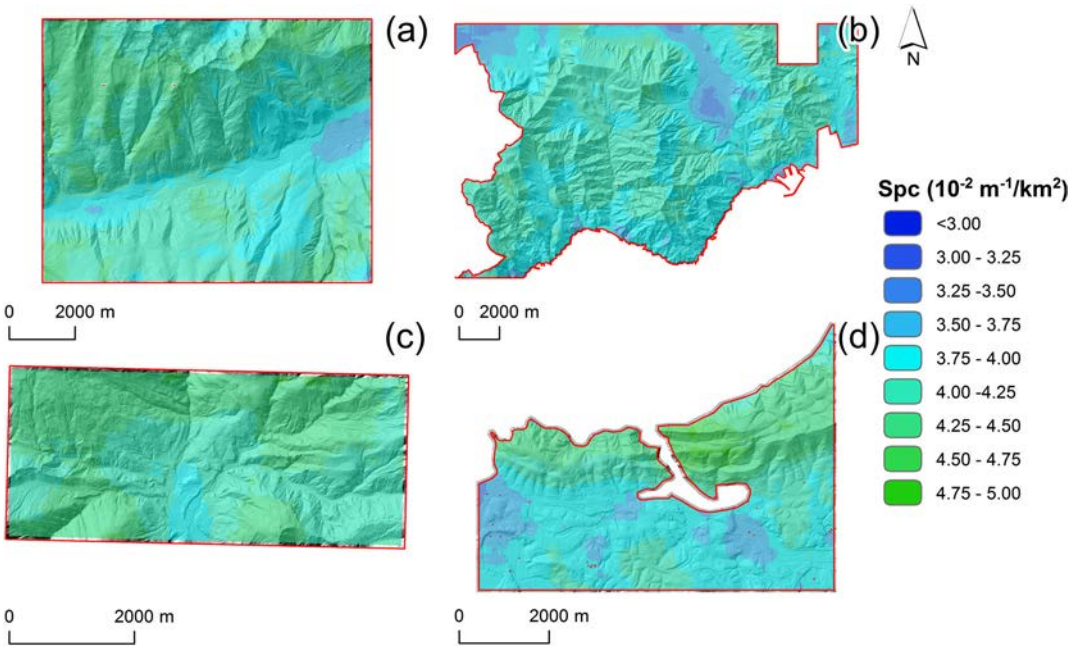

Figure 8. Spc map for the Trento (a), Salerno (b), Paularo (c) and Gipuzkoa (d) study sites. This figure is available in colour online at wileyonlinelibrary.com/journal/espl

Overall, the quality is high if compared with other works about feature extraction, where an average quality of 0.3 was shown (Tarolli *et al.*, 2012; Lin *et al.*, 2013). Considering all four study cases, the hypothesis that maximizes the average SLLAC and minimizes the Spc (maximize ($\overline{SLLAC}$) OR minimize (Spc)) works better than the others in identifying anthropogenic morphologies (presenting at least some road network density or urban complexity). For this combination, the average quality is the highest when considering the overlapping with the network density, the UCI and the NS.

This confirms the hypothesis earlier that the presence of anthropogenic structures determines a morphology that is either well organized (low Spc), less organized but self-similar at a longer distance (high average SLLAC) or both. However, the use of the Spc alone also gives good results (the average quality is the second higher one, after the 'OR' combination). This confirms the findings of Sofia *et al.* (2014b) and Chen *et al.* (2015): anthropogenic elements result in a more organized landscape, thus they tend to minimize the Spc. The average SLLAC alone, for these study cases, seems not to be suitable to identify correctly anthropogenic landscapes, providing the lowest average quality value. The combined use of the two parameters simultaneously (maximize ($\overline{SLLAC}$) AND minimize (Spc)) provides better results: only slightly lower than the Spc alone.

Tables I and II show that there is a threshold of detection: the quality is high for areas having a road density greater than at least 3 km/km^2 and an urban complexity greater than 5 pts/km^2. This is in line with what Sofia *et al.* (2014b)

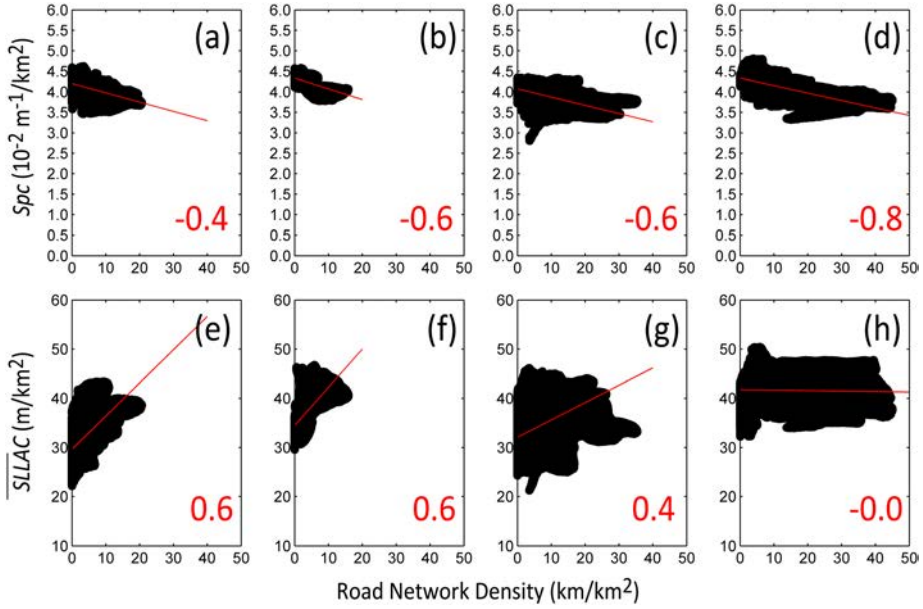

Figure 9. Spc values for the Trento (a), Paularo (b), Salerno (c), and Gipuzkoa (d) study sites, and $\overline{\text{SLLAC}}$ values for the Trento (e), Paularo (f), Salerno (g), and Gipuzkoa (h) study sites as compared to the increase of road density. Pearson's correlation coefficients are shown in red in each plot. This figure is available in colour online at wileyonlinelibrary.com/journal/espl

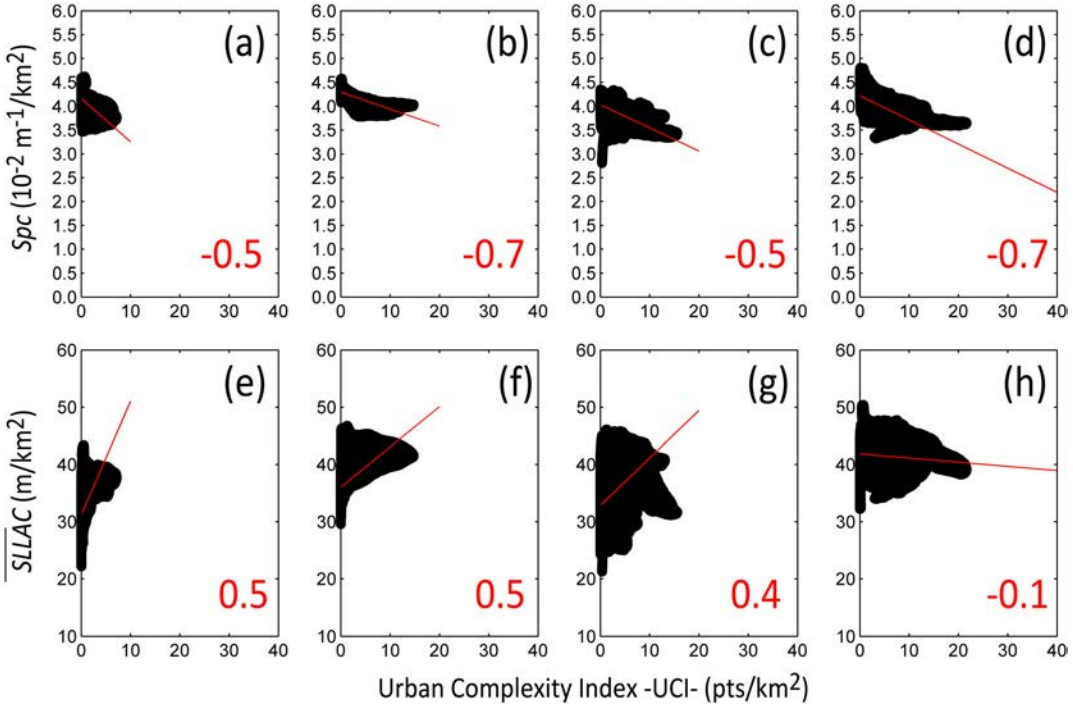

Figure 10. Spc values for the Trento (a), Paularo (b), Salerno (c), and Gipuzkoa (d) study sites, and $\overline{\text{SLLAC}}$ values for the Trento (e), Paularo (f), Salerno (g), and Gipuzkoa (h) study sites as compared to the increase of the Urban Complexity Index (UCI) (road junctions and buildings per km^2). Pearson's correlation coefficients are shown in red in each plot. This figure is available in colour online at wileyonlinelibrary.com/journal/espl

found for terraced areas, where the lower limit of detection was found in relation to the percentage of the terraces' coverage.

Focusing on the different thresholds corresponding to the highest quality, it appears that the different combinations of the parameters (maximize ($\overline{\text{SLLAC}}$) AND minimize (Spc) versus maximize ($\overline{\text{SLLAC}}$) OR minimize (Spc)) capture morphologies influenced by diverse conformations of the network. Table III shows how areas that are correlated at a longer distance and, simultaneously, are well organized (maximize ($\overline{\text{SLLAC}}$) AND minimize (Spc)) mostly correspond to surfaces presenting the most complex networks (NS is low). However, areas that include both complex (yet simple) networks, in addition to the earlier-mentioned regions, include well-organized landscapes (low Spc), but also those less organized but more self-similar (high average SLLAC). The maximize ($\overline{\text{SLLAC}}$) OR minimize (Spc) combination, therefore, also identifies areas having a less complex network, and this is confirmed by the fact that the highest quality is obtained for the highest NS in all study cases.

This, at least in a mountainous hilly context, can also be intended as a geomorphological signature of the two elementary processes regulating the growth and the shape of urban networks: the exploration and the densification of the network (Strano *et al.*, 2012; Corcoran *et al.*, 2013). Regions presenting both exploration and densification tend to be either more organized, in general, or more self-similar (maximize ($\overline{\text{SLLAC}}$) OR

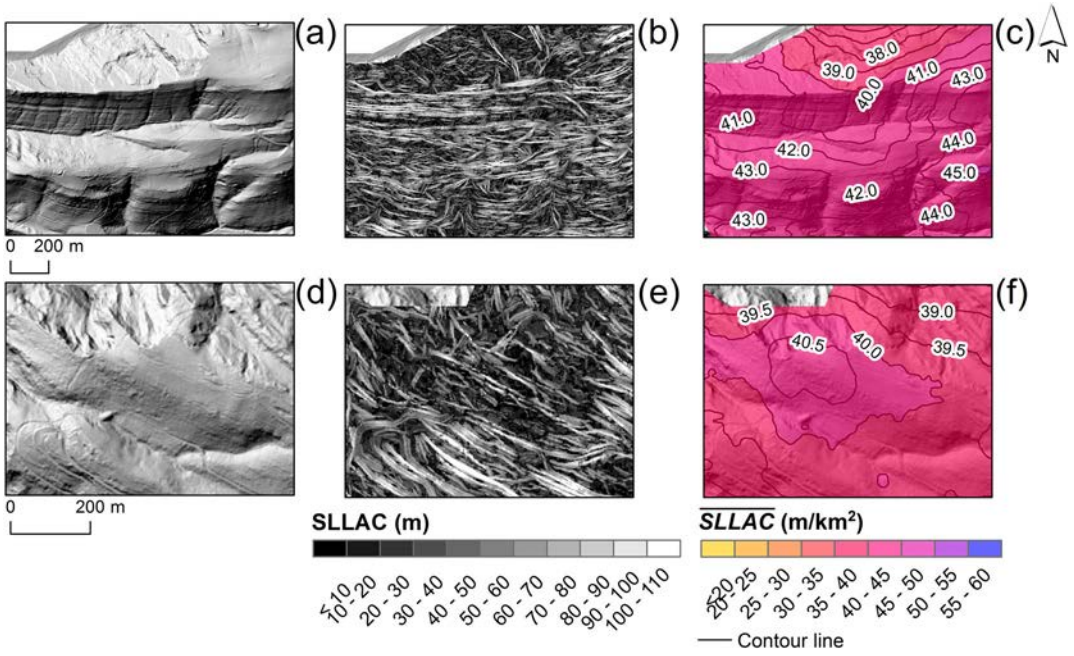

Figure 11. Gipuzkoa study site: example of areas with peculiar morphologies (a and d) that result in fibres on the SLLAC map (b and e), and, consequently, high values of $\overline{\text{SLLAC}}$ (c and f). This figure is available in colour online at wileyonlinelibrary.com/journal/espl

Table I. Maximum quality of extractions compared to different thresholds (Thr) of network density

	Road network density (km/km^2)							
	Maximize (SLLAC) AND minimize (Spc)		Maximize (SLLAC) OR minimize (Spc)		Maximize (SLLAC)		Minimize (Spc)	
	Quality	Thr	Quality	Thr	Quality	Thr	Quality	Thr
Trento	0.5	6.0	0.7	3.0	0.5	2.5	0.6	6.0
Paularo	0.6	5.0	0.6	5.0	0.5	3.0	0.4	5.0
Salerno	0.4	6.0	0.6	3.5	0.6	6.0	0.5	3.5
Gipuzkoa	0.4	5.5	0.8	4.0	0.5	3.5	0.7	7.0
Average	*0.5*	5.6	*0.7*	3.9	*0.5*	3.8	*0.6*	5.4

Table II. Maximum quality of extractions compared to different thresholds (Thr) of the Urban Complexity Index (UCI)

	UCI (pts/km^2)							
	Maximize (SLLAC) AND minimize (Spc)		Maximize (SLLAC) OR minimize (Spc)		Maximize (SLLAC)		Minimize (Spc)	
	Quality	Thr	Quality	Thr	Quality	Thr	Quality	Thr
Trento	0.6	40.0	0.6	5.5	0.6	5.5	0.4	28.5
Paularo	0.8	158.0	0.6	38.5	0.5	31.0	0.4	69.5
Salerno	0.5	68.5	0.7	15.5	0.5	15.0	0.7	71.0
Gipuzkoa	0.4	58.5	0.8	13.0	0.5	11.5	0.8	63.5
Average	*0.6*	81.3	*0.7*	18.1	*0.5*	15.8	*0.6*	58.1

minimize (Spc)), whereas regions with more complex networks are generally well organized and self-similar (maximize ($\overline{\text{SLLAC}}$) AND minimize (Spc)).

Table IV shows the NS computed only considering the road network and the number of junctions and buildings within the cluster that verify the maximize ($\overline{\text{SLLAC}}$) AND minimize (Spc) condition (Cluster$_D$, implying that it is representative of densification networks), and the maximize ($\overline{\text{SLLAC}}$) OR minimize (Spc) condition (Cluster$_M$, implying that it is representative of mixed networks, including densification and exploration networks) for all study cases. In addition, the NS has been computed for those areas (Cluster$_M$) that did not verify maximize ($\overline{\text{SLLAC}}$) AND minimize (Spc) simultaneously (Cluster$_E$), that are, therefore, representative only of exploration networks. The values in Table IV are computed considering the actual network and number of buildings and junctions within the cluster to avoid having part of the area with indefinite values (e.g. KDE for areas with long roads and zero UCI).

In all cases, the Cluster$_M$ presents, in reality, a slightly higher NS than the one verifying maximize ($\overline{\text{SLLAC}}$) AND minimize

Table III. Maximum quality of extractions compared to different thresholds (Thr) of Network Simplicity (network density/Urban Complexity Index)

	Network Simplicity (pts/km)							
	Maximize (SLLAC) AND Minimize (Spc)		Maximize (SLLAC) OR Minimize (Spc)		Maximize (SLLAC)		Minimize (Spc)	
	Quality	Thr	Quality	Thr	Quality	Thr	Quality	Thr
Trento	0.4	0.12	0.6	1.00	0.5	0.77	0.4	0.41
Paularo	0.5	0.03	0.6	1.00	0.4	0.07	0.5	0.04
Salerno	0.4	0.10	0.6	0.29	0.5	0.33	0.5	0.09
Gipuzkoa	0.4	0.11	0.7	0.16	0.4	0.16	0.7	0.11
Average	*0.4*	0.1	*0.6*	0.6	*0.4*	0.3	*0.5*	0.2

Table IV. Network Simplicity computed only considering the road network and the number of junctions and buildings within the cluster that verify the maximize ($\overline{\text{SLLAC}}$) AND minimize (Spc) condition (Cluster_D, implying that it is representative of densification networks), and the maximize ($\overline{\text{SLLAC}}$) OR minimize (Spc) condition (Cluster_M, implying that it is representative of mixed networks, including densification and exploration networks) for all study cases. In addition, the Network Simplicity has been computed for those areas within the Cluster_M that did not verify maximize ($\overline{\text{SLLAC}}$) AND minimize (Spc) simultaneously (Cluster_E), that are, therefore, representative only of exploration networks

	Network Simplicity (10^{-2} pts/km)		
	Cluster_D	Cluster_M	Cluster_E
Trento	5.0	7.8	21
Paularo	1.4	2.2	10
Salerno	1.5	2.1	5
Gipuzkoa	4.3	4.4	5

(Spc), simultaneously (Cluster_D). This confirms what was previously found when analysing Tables I–III, and the different thresholds of network density, UCI and NS. Paularo and Salerno seemed to have similar network conformations in Cluster_D (NS was 1.4 and 1.5 10^{-2} km/pts, respectively). In addition, for these two study sites, the Cluster_M present similar values (NS was 2.2 and 2.1 $\times$ 10^{-2} km/pts, respectively). Similar conclusions can be found for the Cluster_D in Trento and Gipuzkoa, in terms of NS.

However, considering only the part that either maximizes the average SLLAC or minimizes the Spc (Cluster_E), the NS changed. Overall, the Trento area had the most simple exploration network (NS = 20 $\times$ 10^{-2} km/pts), followed by Paularo (NS = 10 $\times$ 10^{-2} km/pts). In the two coastal areas (Salerno and Gipuzkoa), instead, the exploration network presented a more complex structure made of a higher number of short roads (higher number of junctions), and, at the same time, urban areas presented more buildings. Consequently, the NS was lower than that of the alpine sites, but was higher than the NS within Cluster_D. The results of the comparisons between the alpine and coastal sites are in line with what was found in other studies. Urbanization processes in the Alps are not fundamentally different from the processes outside the Alps; however, they occur with a time lag and on a smaller scale (Perlik *et al.*, 2001). Consequentially, the 'exploration' signature is more marked. At the same time, the road signatures on morphology in the Alpine environments reflect the fact that roads here are mostly characterized by a dendritic nature with hierarchical branching, shaped in part by the roads' conformance with valley bottoms and ridges, and by limits due to the slope and the steepness of the terrain (Forman *et al.*, 2003). The exploration signature was slightly less prominent for the considered coastal areas (Gipuzkoa and Salerno), having large cities with a high population density.

Figure 12 shows the Cluster_D (maximize ($\overline{\text{SLLAC}}$) AND minimize (Spc)) and Cluster_M (maximize ($\overline{\text{SLLAC}}$) OR minimize (Spc)) for all study sites. For clarity, Figure 12 also displays the road networks in each study site.

It is interesting to know, especially for the Trento area, that the densification condition ('AND') (Figure 12b) identifies some urban areas also on the hillsides, not only on the valley bottom. In addition, it is interesting that the exploration network is not always visible from the imagery (see, for example, Gipuzkoa, Trento and Paularo in Figure 5). The proposed approach, therefore, being based on LiDAR topography, is able to detect the network conformation also under vegetation cover.

Future challenges, current capabilities and possible utilizations

The average SLLAC and the Spc can be considered a proxy for the road network density, and of the conformation of the morphology (in terms of organization and self-similarity) in a hilly/mountainous context. Understanding the geomorphology of a sloped landscape in relation to the road network not only helps to explain how it evolved to its present form but could also provide an indication of how it will evolve in the future. It could also indicate what hazards or advantages will be created for road construction and what consequences the creation of roads could have on landscape processes.

In the proposed approach, the *k*-means virtually divides the average SLLAC and Spc values into two groups, thus dividing the area into two sub-regions. The average SLLAC and the Spc can then be considered a proxy for the road network density.

If the region was completely anthropogenic, the areas that do not verify maximize ($\overline{\text{SLLAC}}$) OR minimize (Spc) are where the human presence is less evident and leaves a lower signature on the morphology. Networks of roads interact with water and sediment flow paths in multiple ways (Wemple *et al.*, 1996; Jones *et al.*, 2000; Forman *et al.*, 2003), and roads influence a variety of hydrologic and geomorphic processes (Reid and Dunne, 1984; Luce and Cundy, 1994; Montgomery, 1994). These effects vary depending on the network conformation and location with respect to sediment sources, water fluxes and network density. Quantifying the morphological impact of roads and comparing it in terms of different road network

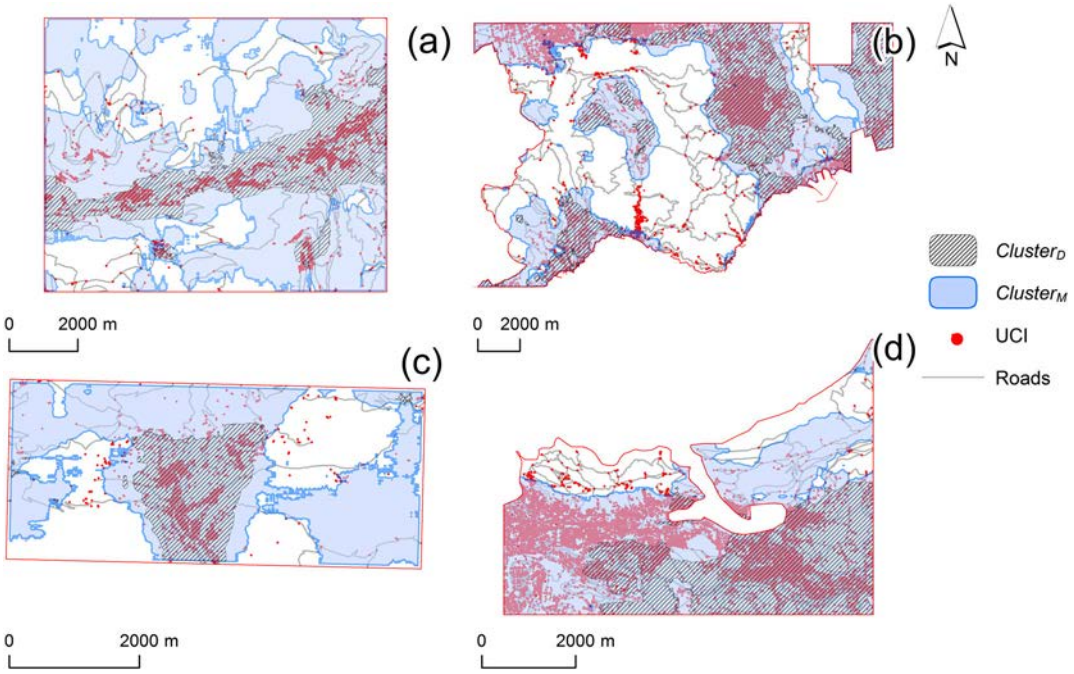

Figure 12. Densification cluster Cluster$_D$ (maximize ($\overline{SLLAC}$) AND minimize (Spc)) and mixed cluster (Cluster$_M$, maximize ($\overline{SLLAC}$) OR minimize (Spc)) for all study sites. For clarity, the figure also displays the road network, junctions and buildings (Urban Complexity Index, UCI) in each study site. This figure is available in colour online at wileyonlinelibrary.com/journal/espl

conformations (or the absence of road networks) could help in understanding the connected processes. At the same time, having multi-temporal LiDAR surveys, it could be possible to track changes over time, gathering observations in diverse environments/conditions.

Among the natural morphologies, those areas more self-similar and more organized (verifying maximize ($\overline{SLLAC}$) OR/AND minimize (Spc)) might be more easily modifiable by humans. Although the spatial configuration of urban landscapes is as much a reflection of the past as it is an indicator of current socio-economic processes and interactions (Seto and Fragkias, 2005), underpinning the physical structures and locational patterns of urban landscapes are transportation networks and the morphology of the landscape. For instance, settlements could gradually extend over unproductive lands with low slope variability, and roads could be created taking advantage of low slopes (Luce and Wemple, 2001).

The results of the previous sections showed that anthropogenic elements, such as road networks, create a different organization of the landscape and the morphology when compared to a natural landscape. This is true in hilly landscapes, but it is potentially true also for a completely flat landscape. On a flat natural site, changes in slope follows generally the landscape forcing, but slope could be inherently self-similar over a long distance (high correlation length, thus, potentially high average SLLAC). However, in flat, low relief anthropogenic landscapes, morphology is hardly modified by road networks, ridges and furrows created by tillage and drainage-irrigation canals (Carluer and Marsily, 2004; Fabian, 2012; Lewin, 2014). These elements are well captured by LiDAR data (Cazorzi *et al.*, 2013; Sofia *et al.*, 2014a). In these low relief contexts, anthropogenic areas could be expected to have at least a higher organization when compared to more natural areas. Further testing should be done to discover if the procedure would work when comparing a flat landscape with only a few roads with a natural mountainous landscape, or analysing a flat landscape, such as the one in Veneto (north Italy) (Fabian, 2012; Sofia *et al.*, 2014c), where there is almost no 'natural' area anymore.

Another aspect to consider is the scale of analysis. While the scale of the template and of the kernel used to compute the SLLAC are robust enough for an overall assessment in different morphological contexts, Borruso (2003) underlined that it is

Table V. Maximum quality of extractions compared to different thresholds (Thr) of the Urban Complexity Index (UCI) computed using a moving window of 200 m for the average SLLAC and Spc, and 100 m for the Kernel Density Estimation (KDE) bandwidth. The average values obtained using a 500 m bandwidth for the KDE and a 1 km^2 moving window for the SLLAC and Spc are also shown for comparison

	Network Simplicity (pts/km)							
	Maximize (SLLAC) AND minimize (Spc)		Maximize (SLLAC) OR minimize (Spc)		Maximize (SLLAC)		Minimize (Spc)	
	Quality	Thr	Quality	Thr	Quality	Thr	Quality	Thr
Trento	0.4	1.00	0.2	2.00	0.3	1.00	0.2	1.00
Paularo	0.4	0.24	0.4	2.84	0.4	2.14	0.4	1.00
Salerno	0.5	1.07	0.6	7.71	0.5	5.54	0.6	1.70
Gipuzkoa	0.3	0.49	0.7	3.17	0.4	3.12	0.6	0.42
Average (100 m versus 200 m)	*0.4*	0.7	*0.5*	3.9	*0.4*	2.9	*0.5*	1.0
Average (500 m versus 1 km^2)	*0.4*	0.1	*0.6*	0.6	*0.4*	0.3	*0.5*	0.2

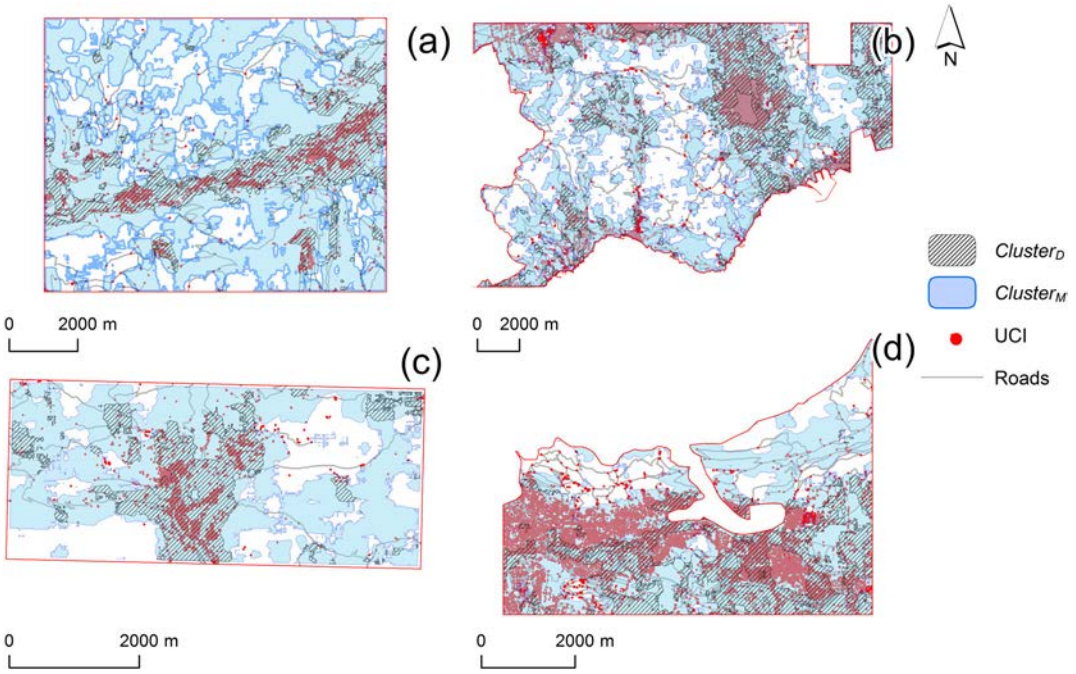

Figure 13. Densification cluster Cluster$_D$ (maximize ($\overline{SLLAC}$) AND minimize (Spc)) and mixed cluster (Cluster$_M$, maximize ($\overline{SLLAC}$) OR minimize (Spc)) for all study sites extracted considering a 200 m moving window to compute the $\overline{SLLAC}$ and the Spc. For clarity, the figure also displays the road network, junctions and buildings (Urban Complexity Index, UCI) in each study site. This figure is available in colour online at wileyonlinelibrary.com/journal/espl

possible to study different urban spatial phenomena, such as medium- and small-sized cities, by changing the KDE bandwidth to estimate the road density (and, in this work, the urban complexity). If one would eventually do so, the size of the window used to evaluate the average SLLAC and the Spc should be changed as well, because this measure should be equivalent to the bandwidth to be able to compare correctly the effects of urban areas and road density on the morphology and the indices derived with the KDE. As an example, for the different study sites, we computed the UCI and the road network density using a bandwidth of 100 m. We then derived the NS index and we compared these maps to the Spc and average SLLAC computed using a moving window of 200 m. Table V shows the maximum qualities obtained, as compared to the quality and thresholds of NS (network density/UCI) obtained with the 1 km^2 window versus 500 m bandwidth.

Changing the size of the windows only slightly reduces the average quality of the extractions. However, the quality values should be considered as a relative measurement to compare the different combination of the parameters, not as an absolute value (Tarolli *et al.*, 2012). What we can understand from this comparison is that reducing the bandwidth and the moving window used to evaluate the Spc and the average SLLAC, with the best extraction, it is possible to capture areas having a different urban/road network complexity and, thus, a different NS. This is in line with the findings of Borruso (2003). In addition, focusing on the combination of parameters that allows for the detection of different network developments (AND for densification networks, and OR for mixed), the differences remain: the OR condition always captures road networks that are simpler.

Figure 13 shows the Cluster$_D$ (maximize ($\overline{SLLAC}$) AND minimize (Spc)) and Cluster$_M$ (maximize ($\overline{SLLAC}$) OR minimize (Spc)) for all study sites considering the 200 m moving window. For clarity, Figure 13 also displays the road networks in each study site.

A visual assessment of Figure 13 confirms what is expressed in Table V. It appears that reducing the moving window used to compute the Spc and the average SLLAC marginally worsen the results for exploration networks, but slightly improves the results for densification networks. As a general research line, these results confirm that the use of a 1 km^2 moving window to compute the Spc and the average SLLAC is, in general, suitable as a first-step detection of anthropogenic morphologies. Changes in the window might characterize, in a second step, densification networks more accurately.

Conclusions

This work tested the SLLAC in relation to anthropogenic elements, such as road network density and urban area complexity, and then applied SLLAC derived parameters to identify automatically anthropogenic geomorphologies. The results show that the presence of a dense road network and urban areas leaves a specific signature on the morphology that is captured by the SLLAC. Long roads and urban area footprints determine the creation of fibres on the SLLAC that are similar to the ones already registered for terraced landscapes. The mean SLLAC per km^2 has a direct correlation with the network density and urban complexity, while the Spc of SLLAC has an inverse correlation with the same parameters. The latter result is in line with Sofia *et al.* (2014b). The proposed method is able to capture the geomorphological signature of two elementary processes regulating the growth and the shape of urban networks: the exploration and the densification of the network. Regions presenting both exploration and densification tend to be either more organized, in general, or more self-similar (high average SLLAC OR low Spc), whereas regions with more complex networks are generally well organized and self-similar at the same time (maximizing the average SLLAC and simultaneously minimizing the Spc). In general, the use of the average SLLAC per km^2 and Spc in a logical disjunction (areas with high average SLLAC, low Spc or both) correctly identifies anthropogenic landscapes in different morphological contexts, as long as they present a road density greater than 3 km/km^2. This latter result is promising for the use of such procedures in areas where roads and anthropogenic morphologies are covered by

vegetation or cannot be seen directly from orthophoto or satellite images. Land management is not sustainable without fully accounting for the impacts of roads and man-made networks on morphology, and a thorough picture of their signature on geomorphology could be useful for the proper design and maintenance of road networks and the analysis of the connected processes.

Acknowledgements—Resources for data analysis were provided by the Interdepartmental Research Centre of Geomatics – CIRGEO at the University of Padova. LiDAR data for the Salerno study area were provided by the Ministry for Environment, Land and Sea (Ministero dell'Ambiente e della Tutela del Territorio e del Mare, MATTM) as part of the 'Extraordinary Plan of Environmental Remote Sensing' (Piano Straordinario di Telerilevamento Ambientale, PST-A) framework. The LiDAR data for the Trento area were provided by the Autonomous Province of Trento (Provincia Autonoma di Trento). The LiDAR DTMs for the Gipuzkoa study site were provided by the Diputacion Foral de Gipuzkoa.

References

Ahnert F. 1988. *Introduction to Geomorphology*. Arnold: London.

Baas ACW, Nield JM. 2007. Modelling vegetated dune landscapes. *Geophysical Research Letters* **34**: L06405. DOI: 10.1029/2006GL029152

Borruso G. 2003. Network density and the delimitation of urban areas. *Transactions in GIS* **7**: 177–191. DOI: 10.1111/1467-9671.00139

Brath A, Montanari A, Moretti G. 2006. Assessing the effect on flood frequency of land use change via hydrological simulation (with uncertainty). *Journal of Hydrology* **324**: 141–153. DOI: 10.1016/j.jhydrol.2005.10.001

Brown AG, Tooth S, Chiverrell RC, Rose J, Thomas DSG, Wainwright J, Bullard JE, Thorndycraft VR, Aalto R, Downs P. 2013. The Anthropocene: is there a geomorphological case? *Earth Surface Processes and Landforms* **38**: 431–434. DOI: 10.1002/esp.3368

Carluer N, Marsily G De, 2004. Assessment and modelling of the influence of man-made networks on the hydrology of a small watershed: implications for fast flow components, water quality and landscape management. *Journal of Hydrology* **285**: 76–95. DOI: 10.1016/j.jhydrol.2003.08.008

Cavalli M, Trevisani S, Goldin B, Mion E, Crema S, Valentinotti R. 2013. Semi-automatic derivation of channel network from a high-resolution DTM: the example of an Italian alpine region. *European Journal of Remote Sensing* **46**: 152–174. DOI: 10.5721/EuJRS20134609

Cazorzi F, Dalla Fontana G, De Luca A, Sofia G, Tarolli P. 2013. Drainage network detection and assessment of network storage capacity in agrarian landscape. *Hydrological Processes* **27**: 541–553. DOI: 10.1002/hyp.9224

Chen J, Li K, Chang K, Sofia G, Tarolli P. 2015. Open-pit mining geomorphic feature characterisation. *International Journal of Applied Earth Observation and Geoinformation* **42**: 76–86. DOI: 10.1016/j.jag.2015.05.001

Coates DB. 1984. Urban geomorphology. In *Applied Geology*. Springer: New York; 601–605.

Collins AL, Walling DE, Stroud RW, Robson M, Peet LM. 2010. Assessing damaged road verges as a suspended sediment source in the Hampshire Avon catchment, southern United Kingdom. *Hydrological Processes* **24**: 1106–1122. DOI: 10.1002/hyp.7573

Corcoran P, Mooney P, Bertolotto M. 2013. Analysing the growth of OpenStreetMap networks. *Spatial Statistics* **3**: 21–32.

Cots-Folch R, Martinez-Casasnovas JA, Ramos MC. 2006. Land terracing for new vineyard plantations in the north-eastern Spanish Mediterranean region: landscape effects of the EU Council Regulation policy for vineyards' restructuring. *Agriculture, Ecosystems & Environment* **115**: 88–96. DOI: 10.1016/j.agee.2005.11.030

Cuff D. 2008. *Anthropogeomorphology*. Oxford *Companion to Global Change*. Oxford University Press: Oxford.

David A, Vassilvitski S. 2007. K-means++: the advantages of careful seeding. In *Proceedings of the Eighteenth Annual ACM-SLAM Symposium on Discrete Algorithms, January 7–9, 2007, New Orleans, LA*; 1027–1035.

Dietrich WE, Perron JT. 2006. The search for a topographic signature of life. *Nature* **439**: 411–418. DOI: 10.1038/nature04452

Djokic D, Maidment DR. 1991. Terrain analysis for urban stormwater modelling. *Hydrological Processes* **5**: 115–124. DOI: 10.1002/hyp.3360050109

Drăguț L, Eisank C, Strasser T. 2011. Local variance for multi-scale analysis in geomorphometry. *Geomorphology* **130**: 162–172.

Ellis EC, Kaplan JO, Fuller DQ, Vavrus S, Klein Goldewijk K, Verburg PH. 2013. Used planet: a global history. *Proceedings of the National Academy of Sciences USA* **110**: 7978–7985.

Ellis EC, Klein Goldewijk K, Siebert S, Lightman D, Ramankutty N. 2010. Anthropogenic transformation of the biomes, 1700 to 2000. *Global Ecology and Biogeography* **19**: 589–606. DOI: 10.1111/j.1466-8238.2010.00540.x

Ellis EC, Ramankutty N. 2007. Putting people in the map: anthropogenic biomes of the world. *Frontiers in the Ecology and the Environment* **6**: 439–447. DOI: 10.1890/070062

European Commission. 2000. Directive 2000/60/EC of the European Parliament and the Council of 23 October 2000 establishing a framework for Community action in the field of water. *Official Journal of the European Communities* **L**: 1–72.

European Commission. 2012. *The Common Agricultural Policy a Partnership between Europe and Farmers*. Directorate-General for Agriculture and Rural Development Publications Office of the European Union: Luxembourg.

Evans IS. 1972. General geomorphometry, derivatives of altitude, and descriptive statistics. In *Spatial Analysis in Geomorphology*, Chorley RJ (ed.). Harper & Row: New York; 17–90.

Evans IS. 1979. *An Integrated System of Terrain Analysis and Slope Mapping*, Final Report (Report 6) on Grant DA-ERO-591-73-G0040. Department of Geography, University of Durham: Durham.

Fabian L. 2012. Extreme cities and isotropic territories: Scenarios and projects arising from the environmental emergency of the central Veneto città diffusa. *International Journal of Disaster Risk Science* **3**: 11–22. DOI: 10.1007/s13753-012-0003-5

Forman RTT. 2000. Estimate of the area affected ecologically by the road system in the United States. *Conservation Biology* **14**: 31–35. DOI: 10.1046/j.1523-1739.2000.99299

Forman RTT, Sperling D, Bissonette JA, Clevenger AP, Cutshall CD, Dale VH, Fahrig L, France R, Goldman CR, Heanue K, Jones JA, Swanson FJ, Turrentine T, Winter TC. 2003. *Road Ecology: Science and Solutions*. Island Press: Washington, DC.

Gatrell A. 1994. Density estimation and the visualisation of point patterns. In *Visualisation in Geographical Information Systems*, Hearnshaw HM, Unwin D (eds). John Wiley & Sons: Chichester; 65D75

Diputacion Foral de Gipuzkoa. 2005. *Servicio de Cartografía*. Dirección de Ordenación del Territorio; Departamento de M. Ambiente, Planificación Territorial, Agricultura y Pesca. Gobierno Vasco. http://b5m.gipuzkoa.net/url5000/es/G_22485/PUBLI&consulta=HAZLIDAR [January 12, 2014].

Gironás J, Niemann J, Roesner L, Rodriguez F, Andrieu H. 2009. Evaluation of Methods for Representing Urban Terrain in Storm-Water Modeling. *Journal of Hydrologic Engineering* **15**: 1–14. DOI: 10.1061/(ASCE)HE.1943-5584.0000142

Gucinski H, Furniss MJ, Ziemer RR, Brookes MH. 2001. *Forest Roads: A Synthesis of Scientific Information*, General Technical Report PNW-GTR-509. US Department of Agriculture, Pacific Northwest Research Station: Portland, OR.

Haff PK. 2010. Hillslopes, rivers, plows, and trucks: mass transport on Earth's surface by natural and technological processes. *Earth Surface Processes and Landforms* **35**: 1157–1166. DOI: 10.1002/esp.1902

Haggett P, Chorley RJ. 1996. *Network Analysis in Geography*. Edward Arnold: London.

Hailemariam FM, Brandimarte L, Dottori F. 2014. Investigating the influence of minor hydraulic structures on modeling flood events in lowland areas. *Hydrological Processes* **28**: 1742–1755. DOI: 10.1002/hyp.9717

Haralick RM, Shapiro LD. 1992. *Computer and Robot Vision*, 2 vols. Addison Wesley: Reading, MA.

Heipke C, Mayer H, Wiedemann C, Jamet O. 1997. Automated reconstruction of topographic objects from aerial images using vectorized map information. *International Archives of Photogrammetry and Remote Sensing* **23**: 47–56.

Hooke RL. 2000. On the history of human as geomorphic agents. *Geology* **28**: 843–846. DOI: 10.1130/0091-7613(2000)28<843:OTHOHA>2.0.CO

Institut Cartografic de Catalunya (ICC). 2005. *Informe del levantamiento lidar del Territorio Historico de Gipuzkoa*, ICC Barcelona.

Institut Cartographic de Catalunya (ICC). 2008. *Informe final del proyecto MDT LiDAR del Territorio Historico de Gipuzkoa*. ICC: Barcelona.

ISO. 2013a. *ISO 25178-2:2013: Geometrical Product Specifications (GPS) – Surface Texture: Areal — Part 2: Terms, Definitions and Surface Texture Parameters*. ISO: London.

ISO. 2013b. *ISO 2178-3:2013: Geometrical Product Specifications (GPS) – Surface Texture: Areal – Part 3: Specification Operators*. ISO: London.

Jefferson AJ, Wegmann KW, Chin A. 2013. Geomorphology of the anthropocene: understanding the surficial legacy of past and present human activities. *Anthropocene* **2**: 1–3. DOI: 10.1016/j.ancene.2013.10.005

Jones DK, Baker ME, Miller AJ, Jarnagin ST, Hogan DM. 2014. Tracking geomorphic signatures of watershed suburbanization with multitemporal LiDAR. *Geomorphology* **219**: 42–52. DOI: 10.1016/j.geomorph.2014.04.038

Jones JA, Swanson FJ, Wemple BC, Snyder KU. 2000. Effects of roads on hydrology, geomorphology, and disturbance patches in stream networks. *Conservation Biology* **14**: 76–85. DOI: 10.1046/j.1523-1739.2000.99083.x

Jordan H, Hamilton K, Lawley R, Price SJ. 2014. *Anthropogenic contribution to the geological and geomorphological record: a case study from Great Yarmouth, Norfolk, UK*. Geomorphology. DOI: 10.1016/j.geomorph.2014.07.008

Katz HA, Daniels JM, Ryan S. 2014. Slope-area thresholds of road-induced gully erosion and consequent hillslope–channel interactions. *Earth Surface Processes and Landforms* **39**: 285–295. DOI: 10.1002/esp.3443

Khonsari MME, Booser R. 2008. *Applied Tribology: Bearing Design and Lubrication*, 2nd edn. John Wiley & Sons: Chichester.

Krause S, Jacobs J, Bronstert A. 2007. Modelling the impacts of land-use and drainage density on the water balance of a lowland–floodplain landscape in northeast Germany. *Ecological Modelling* **200**: 475–492. DOI: 10.1016/j.ecolmodel.2006.08.015

Lewin J. 2014. The English floodplain. *Geographical Journal* **180**: 317–325. DOI: 10.1111/geoj.12093

Lewin J, Macklin MG. 2014. Marking time in geomorphology: should we try to formalise an anthropocene definition? *Earth Surface Processes and Landforms* **39**: 133–137. DOI: 10.1002/esp.3484

Lewis JP. 1995. Fast template matching. *Vision Interface* **95**: 120–123.

Lin C-W, Tseng C-M, Tseng Y-H, Fei L-Y, Hsieh Y-C, Tarolli P. 2013. Recognition of large scale deep-seated landslides in forest areas of Taiwan using high resolution topography. *Journal of Asian Earth Sciences* **62**: 389–400. DOI: 10.1016/j.jseaes.2012.10.022

Lloyd S. 2006. Least squares quantization in PCM. *IEEE Transactions on Information Theory* **28**: 129–137. DOI: 10.1109/TIT.1982.1056489

Luce CH, Cundy TW. 1994. Parameter identification for a runoff model for forest roads. *Water Resources Research* **30**: 1057–1069. DOI: 10.1029/93WR03348

Luce CH, Wemple BC. 2001. Introduction to special issue on hydrologic and geomorphic effects of forest roads. *Earth Surface Processes and Landforms* **26**: 111–113. DOI: 10.1002/1096-9837(200102)26:2<111::AID-ESP165>3.0.CO;2-2

Montgomery DR. 1994. Road surface drainage, channel initiation, and slope instability. *Water Resources Research* **30**: 1925–1932. DOI: 10.1029/94WR00538

Nyssen J, Poesen J, Moeyersons J, Luyten E, Veyret-Picot M, Deckers J, Haile M, Govers G. 2002. Impact of road building on gully erosion risk: a case study from the Northern Ethiopian Highlands. *Earth Surface Processes and Landforms* **27**: 1267–1283. DOI: 10.1002/esp.404

OpenStreetMap. 2014. Geofabrik's Free Download Server. http://download.geofabrik.de/europe.html [January 12, 2014].

Pacione M. 1987. Socio-spatial development of the South Italian city: the case of Naples. *Transactions of the Institute of British Geographers* **12**: 433–450. DOI: 10.2307/622794

Passalacqua P, Belmont P, Foufoula-Georgiou E. 2012. Automatic geomorphic feature extraction from lidar in flat and engineered landscapes. *Water Resources Research* **48**: W03528. DOI: 10.1029/2011WR010958

Pearson K. 2006. Note on regression and inheritance in the case of two parents. *Proceedings of the Royal Society London* **58**: 240–242. DOI: 10.1098/rspl.1895.0041

Penna D, Borga M, Aronica GT, Brigandì G, Tarolli P. 2014. The influence of grid resolution on the prediction of natural and road-related shallow landslides. *Hydrology and Earth System Sciences* **18**: 2127–2139. DOI: 10.5194/hess-18-2127-2014

Perlik M, Messerli P, Batzing W. 2001. Towns in the Alps: urbanization processes, economic structure, and demarcation of European functional urban areas (EFUAs) in the Alps. *Mountain Research and Development* **21**: 243–252. DOI: 10.1659/0276-4741(2001)021[0243:TITA]2.0.CO;2

Phillips JD. 1992. Nonlinear dynamical systems in geomorphology: revolution or evolution? *Geomorphology* **5**: 219–229. http://dx.doi.org/10.1016/0169-555X(92)90005-9

Prosdocimi M, Calligaro S, Sofia G, Dalla Fontana G, Tarolli P. 2015. Bank erosion in agricultural drainage networks: new challenges from Structure-from-Motion photogrammetry for post-event analysis. *Earth Surface Processes and Landforms*. DOI: 10.1002/esp.3767

Reid L, Dunne T, Cederholm C. 1981. Application of sediment budget studies to the evaluation of logging road impact. *Journal of Hydrology* **20**: 49–62.

Reid LM, Dunne T. 1984. Sediment Production From Forest Road Surfaces. *Water Resources Research* **20**: 1753–1761. DOI: 10.1029/WR020i011p01753

Rodriguez-Iturbe I, Rinaldo A. 1997. Fractal river basins: chance and self-organization. Cambridge University Press.

Rózsa P. 2010. Nature and extent of human geomorphological impact: a review. In *Anthropogenic Geomorphology: A Guide to Man-made Landforms*, Szabo J, David L, Loczy D (eds). Springer: New York; 273–290.

Schmidt J, Evans IS, Brinkmann J. 2003. Comparison of polynomial models for land surface curvature calculation. *International Journal of Geographical Information Science* **17**: 797–814. DOI: 10.1080/1365881031000159605 8

Seto KC, Fragkias M. 2005. Quantifying spatiotemporal patterns of urban land-use change in four cities of China with time series landscape metrics. *Landscape Ecolology* **20**: 871–888. DOI: 10.1007/s10980-005-5238-8

Sheppard RJ. 2000. Laser-scanning for landscape planning: implications for policy and practice from an end-user's perspective. *International Archives of Photogrammetry and Remote Sensing and Spatial Information Sciences XXXVI-8/W2*.

Sidle RC, Ziegler AD. 2012. The dilemma of mountain roads. *Nature Geoscience* **5**: 437–438. DOI: 10.1038/ngeo1512

Silverman BW. 1988. *Density Estimation for Statistics and Data Analysis*. Chapman and Hall: New York.

Sofia G, Dalla Fontana G, Tarolli P. 2014a. High-resolution topography and anthropogenic feature extraction: testing geomorphometric parameters in floodplains. *Hydrological Processes* **28**: 2046–2061. DOI: 10.1002/hyp.9727

Sofia G, Marinello F, Tarolli P. 2014b. A new landscape metric for the identification of terraced sites: the Slope Local Length of Auto-Correlation (SLLAC). *ISPRS Journal of Photogrammetry and Remote Sensing* **96**: 123–133. DOI: 10.1016/j.isprsjprs.2014.06.018

Sofia G, Pirotti F, Tarolli P. 2013. Variations in multiscale curvature distribution and signatures of LiDAR DTM errors. *Earth Surface Processes and Landforms* **38**: 1116–1134. DOI: 10.1002/esp.3363

Sofia G, Prosdocimi M, Dalla Fontana G, Tarolli P. 2014c. Modification of artificial drainage networks during the past half-century: evidence and effects in a reclamation area in the Veneto floodplain (Italy). *Anthropocene* **6**: 48–62. DOI: 10.1016/j.ancene.2014.06.005

Sofia G, Tarolli P, Cazorzi F, Dalla Fontana G. 2015. Downstream hydraulic geometry relationships: gathering reference reach-scale width values from LiDAR. *Geomorphology* **250**: 236–248. DOI: 10.1016/j.geomorph.2015.09.002

Steffen W, Crutzen J, McNeill JR. 2007. The anthropocene: are humans now overwhelming the great forces of nature? *Ambio* **36**: 614–621. DOI: 10.1579/0044-7447(2007)36[614:TAAHNO]2.0.CO;2

Stout KJ, Sullivan PJ, Dong WP, Mainsah E, Luo N, Mathia T, Zahouani H. 1994. *The Development of Methods for the*

Characterization of Roughness on Three Dimensions. Butterworth-Heinemann: Oxford.

Strano E, Nicosia V, Latora V, Porta S, Barthélemy M. 2012. Elementary processes governing the evolution of road networks. *Scientific Reports* **2**(296). DOI: 10.1038/srep00296

Szabo J. 2010. Anthropogenic geomorphology: subject and system. In *Anthropogenic Geomorphology: A Guide to Man-made Landforms*, Szabo J, David L, Loczy D (eds). Springer: New York; 3–10.

Tarboton DG, Bras RL, Rodriguez-Iturbe I. 1988. The fractal nature of river networks. *Water Resources Research* **24**: 1317–1322. DOI: 10.1029/WR024i008p01317

Tarolli P. 2014. High-resolution topography for understanding Earth surface processes: opportunities and challenges. *Geomorphology* **216**: 295–312. DOI: 10.1016/j.geomorph.2014.03.008

Tarolli P, Calligaro S, Cazorzi F, Dalla Fontana G. 2013. Recognition of surface flow processes influenced by roads and trails in mountain areas using high-resolution topography. *European Journal of Remote Sensing* **46**: 176–197. DOI: 10.5721/EuJRS20134610

Tarolli P, Sofia G, Calligaro S, Prosdocimi M, Preti F, Dalla Fontana G. 2015. Vineyards in terraced landscapes: new opportunities from lidar data. *Land Degradation and Developement* **26**: 92–102. DOI: 10.1002/ldr.2311

Tarolli P, Sofia G, Dalla Fontana G. 2012. Geomorphic features extraction from high-resolution topography: landslide crowns and bank erosion. *Natural Hazards* **61**: 65–83. DOI: 10.1007/s11069-010-9695-2

Thomas I, Frankhauser P, Biernacki C. 2008. The morphology of built-up landscapes in Wallonia (Belgium): a classification using fractal indices. *Landscape and Urban Planning* **84**: 99–115.

Wemple BC, Jones JA, Grant GE. 1996. Channel network extension by logging roads in two basins, western Cascades, Oregon. *JAWRA Journal of the American Water Resources Association* **32**: 1195–1207. DOI: 10.1111/j.1752-1688.1996.tb03490.x

Whitehouse DJ. 2011. Characterization. In *Handbook of Surface and Nanometrology*, 2nd edn. CRC Press: Boca Raton, FL; 5–170.

Wohl E. 2013. Wilderness is dead: whither critical zone studies and geomorphology in the anthropocene? *Anthropocene* **2**: 4–15. DOI: 10.1016/j.ancene.2013.03.001

Wu J, Qi Y. 2000. Dealing with scale in landscape analysis: an overview. *Geographic Information Sciences: A Journal of the Association of Chinese Professionals in Geographic Information Systems* **6**: 1–5. DOI: 10.1080/10824000009480528

Zalasiewicz J, Williams M, Fortey R, Smith A, Barry TL, Coe AL, Bown PR, Rawson PF, Gale A, Gibbard P, Gregory FJ, Hounslow MW, Kerr AC, Pearson P, Knox R, Powell J, Waters C, Marshall J, Oates M, Stone P. 2011. Stratigraphy of the anthropocene. *Philosophical Transactions of the Royal Society of London A: Mathematical, Physical and Engineering Sciences* **369**: 1036–1055. DOI: 10.1098/rsta.2010.0315